Common characteristics of displacive and relaxor ferroelectrics

Adrian N. Bishop, A. Bussmann-Holder, S. Kamba, Mario Maglione

Common characteristics of displacive and relaxor ferroelectrics

A. R. Bishop,[1] A. Bussmann-Holder,[2] S. Kamba,[3] and M. Maglione[4]
[1]*Los Alamos National Laboratory, Los Alamos, New Mexico 87545, USA*
[2]*Max-Planck-Institute for Solid State Research, Heisenbergstr. 1, D-70569 Stuttgart, Germany*
[3]*Institute of Physics ASCR, Na Slovance 2, 182 21 Prague 8, Czech Republic*
[4]*Institut de Chimie de la Matière Condensée de Bordeaux, CNRS, 87 Avenue A. Schweitzer, F-33608 Pessac, France*
(Received 2 December 2009; revised manuscript received 17 January 2010; published 12 February 2010)

The long-standing classification scheme of ferroelectrics into either relaxor or displacive ones (the phase transition is driven by a soft phonon mode) is too restrictive since a smooth crossover between them exists which even admits for a coexistence of both phenomena. This crossover and coexistence is a consequence of the varying density of polar nanoregions due to different doping levels of the respective system. The formation of polar nanoregions is attributed here to intrinsic local modes in terms of discrete breathers.

DOI: 10.1103/PhysRevB.81.064106 PACS number(s): 77.80.−e, 77.84.−s

Relaxor ferroelectrics have been studied intensively for many years due to their high potential for applications and technological importance. Early on it was emphasized that their diffuse phase transitions can be related to chemical disorder at the cation lattice site which may cause a spatial distribution of local diffuse phase transitions.[1] Later on it was suggested that nanoscale fluctuating dipoles are formed in an otherwise intact matrix giving rise to polar nanoregions (PNRs).[2–4] Many experiments provide indirect evidence for this scenario,[5] as, e.g., in infrared and broadband dielectric spectroscopy a two-component relaxation is observed, which are related to the flipping and breathing of PNRs.[6–8] From similar experiments it is concluded that the local symmetry of the relaxor state is lower than the average structural one originating from the formation of the PNRs.[6–8] The appearance of diffuse inelastic scattering and the phenomenon of the "waterfall" effect as observed by inelastic neutron scattering (INS) have been speculated to arise from the scattering of transverse acoustic or optic phonons on PNRs at critical wave vector $q=\frac{2\pi}{l}$ where l is the dimension of PNRs.[9–12] This scenario has been questioned and an alternative coupled-mode analysis used to account for the waterfall,[13] Using pulsed neutron inelastic scattering it was concluded that relaxor ferroelectrics are characterized by dynamic local polarization regions which, with decreasing temperature are slowing down, to finally coalesce into PNRs.[14] While the above experimental results have been performed on Pb containing perovskites ABO_3 with either A or B site disorder, $SrTiO_3$ doped with either Ba or Ca and $BaTiO_3$ doped with Sr or Zr show a crossover from soft mode to relaxor behavior with increasing doping.[15,16] This observation suggests that soft mode and relaxor behavior can smoothly merge into each other and may even coexist. Similar conclusions were reached for Li or Nb doped $KTaO_3$, where a coexistence of a dipolar glass behavior with conventional ferroelectricity was observed.[17,18]

While experimentally the PNRs are rather well investigated—even though their existence has only indirectly been established—theoretically no consensus about their microscopic origin has been achieved. It has, however, been established theoretically[19] that the PNRs predominantly form in chemically ordered nanoregions with these regions exhibiting a lower symmetry than the average one. The analogy of relaxors with dipolar glasses[20] has led to the proposal that a random-field Ising model could be appropriate for the description of these compounds.[21] Its extensions to the spherical random bond random-field model[22] is based on the interaction between PNRs and accounts well for the radio frequency response and NMR data on relaxors.[23] For Li doped $KTaO_3$ a microscopic model to explain the relaxor state has been formulated based on the pairwise interaction between neighboring Li ions and a random-field approach.[24–26] However, both of these models[21,22] remain phenomenological and do not provide a microscopic basis for the formation of PNRs. The latter microscopic model[24–26] carries some resemblance with a previous study[27–29] but differs from it since a pairwise interaction is not the cause of the relaxor behavior but rather the formation of local finite-size dipole moments.

Here, we use the strong nonlinearity inherent to these systems and show that intrinsic local mode (ILM) formation in terms of discrete breather solutions cannot only account for the relaxor state but also for the crossover to soft-mode dynamics and their possible coexistence.

Ferroelectric perovskite oxides are inherently highly anharmonic and their dynamics is well characterized by local double-well potentials in the electron-ion interaction.[30,31] Such kind of potentials are responsible for phonon softening and structural instability[30–34] but also carry exact nonlinear solutions which are well suited to describing domain-wall formation and dynamics.[35–37] In addition, breather solutions have recently been shown to exist[27] with finite spatial extensions of these solutions a prerequisite for their stability. These finite and site-dependent solutions are novel as compared to previous results since the double well used in Refs. 27, 30, and 31 differs from typical double wells: it is taken in the polarizability coordinate which is a relative displacement coordinate between the ionic core and its surrounding electronic shell. By treating the relaxor state as a two-component system, the unpolarized intact matrix with average cubic symmetry is modeled within the self-consistent phonon approximation (SPA) with effective temperature-dependent harmonic coupling constants appropriate to describe soft-mode dynamics; the regions surrounding the dopant sites are considered in terms of the ILM solutions. Since the matrix

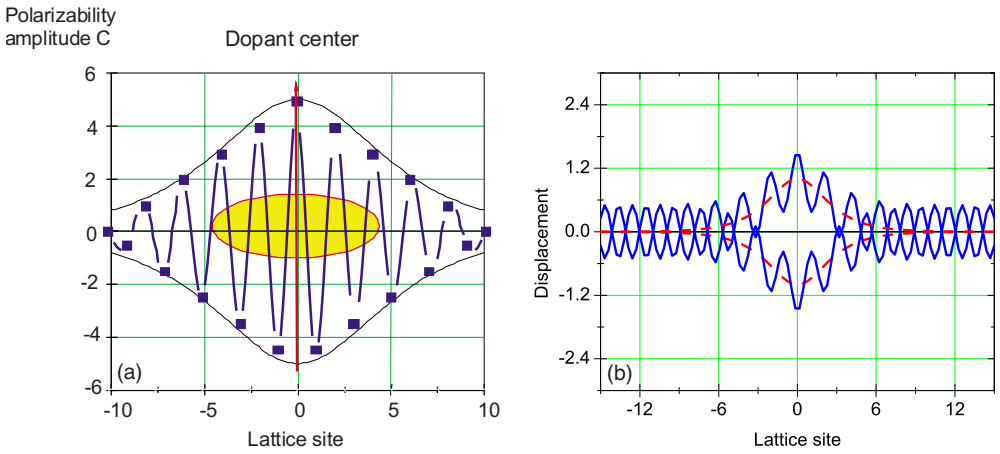

FIG. 1. (Color online) (a) ILM amplitude C as a function of the lattice site. Site 0 refers to the dopant site. (b) Superposition of the ILM and regular lattice displacements as a function of the lattice site where, as in (a) the site 0 is the dopant site.

and ILM dynamics are not independent of each other, a superposition principle of the two types of solutions is used which guarantees coupled dynamics.[27–29] This approach also provides a stabilization mechanism to the matrix by reducing the soft-mode temperature dependence and the ILM solution adopts a temperature dependence.

The model Hamiltonian representing a pseudo-one-dimensional system with polarizable BO_3 cluster ions of mass m_1 and a rigid-ion A sublattice of mass m_2 is given by[27,30,31]

$$H = \frac{1}{2}\sum_{i=1,2,n}\left[m_i\dot{u}_{in}^2 + m_v(\dot{u}_{1n}-\dot{w}_{1n})^2\right] + \frac{1}{2}\sum_n\Bigg[f'(u_{1n}-u_{1n+1})^2 + f(u_{2n}-u_{1n}+w_{1n})^2 + f(u_{2n-1}-u_{1n}+w_{1n})^2 + g_2 w_{1n}^2 + \frac{2}{r}g_4^{(r)}w_{1n}^r\Bigg], \tag{1}$$

where m_v is the BO_3 electronic shell mass (treated in the adiabatic approximation) and u_{in} are the site n-dependent displacements of ion $i=1,2$. w_{1n} is the polarizability coordinate, which is the relative displacement between BO_3 core and the surrounding electronic shell. f, f', g_2 are nearest neighbor, second nearest neighbor, and on-site attractive harmonic coupling constants. r defines the degree of nonlinearity and $g_4^{(r)}$ is repulsive thereby guaranteeing the lattice stability. Typically, $r=4$, leading to a local double-well potential. ILM formation takes place when a constant frequency regime is observed within a spatially limited region of the lattice, being zero everywhere else. To demonstrate the existence of these solutions, time periodic solutions of the following form are assumed: $u_{1n}=A\xi_{1n}\cos(\omega t)$, $u_{2n}=B\xi_{2n}\cos(\omega t)$, $w_{1n}=C\eta_{1n}\cos(\omega t)$, where A, B, C are the amplitudes and ξ, η the related displacements. When doping the ABO_3 matrix, local displacements in the polarizability coordinate take place which differ from those of the matrix. Since this spatially enhanced polarizability creates a local electric field, it has to be compensated by reversed displacements of the nearest-neighbor polarizations [Fig. 1(a)].

The central-atom (doping site) polarizability amplitude C is thus the quantity which controls the breather spatial extent: with C large, the spatial extent is large and with C small, the breather extends only over a few nearest-neighbor lattice sites. In order to simulate doping, the breather amplitude is taken as the relevant quantity where large doping levels are characterized by large amplitudes (caused by the dense doping concentration) while small doping levels correspond to small amplitudes (caused by the dilute dopant distribution). In this way a continuous doping increase is modeled through a continuous increase in C. The constant frequency regime is given by the solutions,

$$\omega_1^2 = \frac{1}{m_1}\left[4f' + g\frac{C}{A}\right]; \quad \omega_2^2 = \frac{2f}{m_2} \tag{2}$$

with $g=2g_2+C_r\tilde{g}_4C^2$, $\tilde{g}_4^{(n)}=g_4/(n-n_c)$, and $C_r\cos(\omega t)=\cos^{r-1}(\omega t)$. n_c is the lattice site at which the breather amplitude is zero. Note that the solution for $n_c=1$ is unstable. Also, note that the site dependence of $\tilde{g}_4$ introduces site-dependent double-well potentials and correspondingly a distribution of dipole moments within the breather spatial extent. This implies that within the ILM, inhomogeneity controls the dynamics. Since breather solutions are only stable in a frequency regime of the system's characteristic phonon frequencies, ω_2^2 can be ignored in the following discussion since this frequency coincides with the optic mode zone-boundary frequency.

The interaction between the ILM and the surrounding matrix is provided by the superposition of the corresponding displacement coordinates according to $u=u_{matrix}+u_{\mathrm{ILM}}$ [Fig. 1(b). While the average dynamics remain unaffected by this superposition, local dynamics change considerably. This has also been observed by static[38] and dynamic[14,15] pair distribution function (PDF) experiments. The major effect is, however, that the ILM becomes temperature dependent, whereas the lattice soft-mode optic frequency $\omega_{f,\mathrm{TO}}(q=0)$ is stabilized. This stabilization depends on the ILM amplitude C, where large values of it almost suppress any temperature dependence of $\omega_{f,\mathrm{TO}}(q=0)$, whereas small amplitudes leave a temperature regime for mode softening and freezing. Within

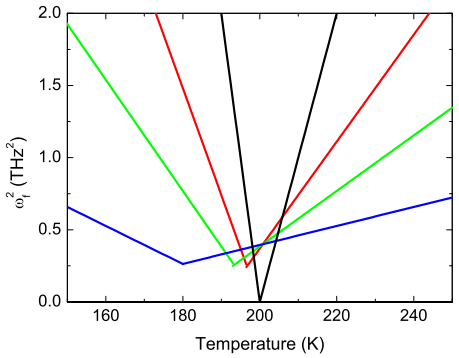

FIG. 2. (Color online) Temperature dependence of the squared soft-mode frequency without ILM renormalization (black) T_c =200 K, small ILM amplitude (red), large ILM amplitude (green), and the extremely dense ILM case (blue).

the above model the squared soft-mode frequency is explicitly given by

$$\omega_{f,\mathrm{TO}}^2(q=0)=\omega_f^2(T)=2f(g_T+3g_4C^2)/[\mu(2f+g_T+3g_4C^2)] \tag{3}$$

with μ being the reduced cell mass and $g_T=-g_2+3g_4\langle w^2\rangle_T$, where $\langle w^2\rangle_T=\Sigma_{q,j}\hbar/(m\omega_{q,j})w_{q,j}^2\coth[\hbar\omega_{q,j}/(2k_BT)]$. ω refers to the momentum q and phonon branch j-dependent eigenfrequencies within the SPA. The ferroelectric transition temperature is given by $\omega_f^2(T_c)=0$. Thereby an implicit relation for T_c can be derived,

$$g_T+3g_4C^2=0,\quad \frac{g_2-3g_4C^2}{3g_4}=\sum_{q,j}\frac{\hbar}{m\omega_{q,j}}w_{q,j}^2\coth\left[\frac{\hbar\omega_{q,j}}{2k_BT_c}\right], \tag{4}$$

which differs from T_c in the purely displacive case, i.e.,

$$\frac{|g_2|}{3g_4}=\sum_{q,j}\frac{\hbar}{m\omega_{q,j}}w_{q,j}^2\coth\left[\frac{\hbar\omega_{q,j}}{2k_BT_c}\right] \tag{5}$$

through the stabilization of the attractive term by the ILM amplitude. As such, the ILM modifies T_c since the attractive core-shell interaction is reduced with increasing breather amplitude, i.e., increasing doping. This can lead to a complete stabilization of the soft-mode frequency. On the other hand, in the dilute limit, T_c is reduced as compared to the undoped case but a phase transition can still occur, as is obvious from Eq. (4). However, a complete softening of ω_f^2 is inhibited since in the limit $g_T\to 0$ ω_f^2 remains pinned through the ILM at $\omega_f^2=6fg_4C^2/[\mu(2f+3g_4C^2)]$. This incomplete softening has been observed in a variety of relaxors[6,39–41] and has been attributed to the breaking of percolated polar clusters.[6]

Below T_c the potential defining parameters have to be replaced by $-2g_2$, $-2g_4$, and $g_T\to -2g_T$.[31] This replacement yields the typical recovery of the soft mode below T_c which hardens with decreasing temperature. In the presence of the ILM this dependence is reduced since now—analogous to the paraelectric phase: $2g_2\to 2g_2+6g_4C^2$. To make things explicit, the temperature dependence of ω_f^2 in the ferroelectric phase is given by

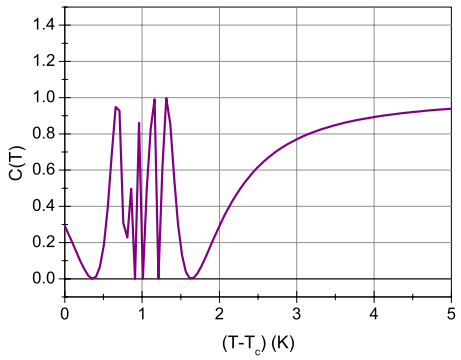

FIG. 3. (Color online) Fluctuation induced renormalized ILM amplitude C [C is implicitly defined in Eq. (7)] in the vicinity of $T=T_c$. The renormalization due to fluctuations is almost lost for $T>T_c+3$ K.

$$\omega_f^2(T\le T_c)=\frac{2f[2g_2-3g_4(2\langle w^2\rangle_T-C^2)]}{\mu[2f+2g_2-3g_4(2\langle w^2\rangle_T-C^2)]}. \tag{6}$$

From Eq. (6) it becomes clear that the soft-mode hardens below T_c but its temperature dependence can be quite different from the case of a displacive ferroelectric caused by the temperature reducing effect from the ILM amplitude. A typical T dependence of $\omega_f^2(T)$ is shown in Fig. 2 where with increasing ILM amplitude the temperature dependence of ω_f^2 is systematically reduced. The Curie constant is substantially suppressed with increasing ILM amplitude as seen experimentally[15,42–45] and outlined in detail below. Below T_c the soft-mode hardens and this hardening gets less pronounced with increasing breather amplitude

The renormalization of the ILM mode caused by the coupling to the matrix modifies Eq. (2) in the following way: if a transition to a polar state (the dilute case) still occurs in the presence of the breather, the breather frequency changes for $T>T_c$ like

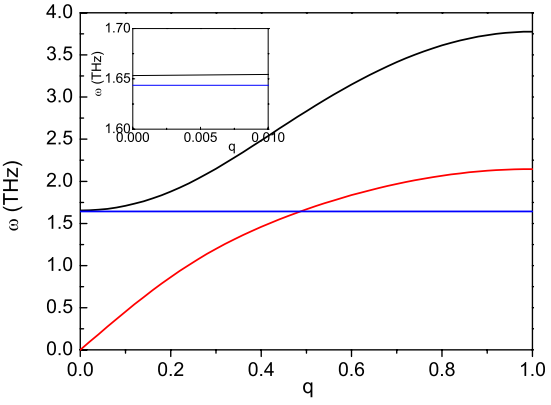

FIG. 4. (Color online) Dispersion branches of the lowest transverse optic (black line) and acoustic (red line) branches below T_B. T_B is the temperature where the ILM branch splits off from the optic branch, i.e., $T\le T_B$. The blue line refers to the ILM. The ILM distribution is dense. The inset shows the small q dispersion of the optic and ILM mode in order to demonstrate the small splitting of both in this regime which is not obvious from the main figure.

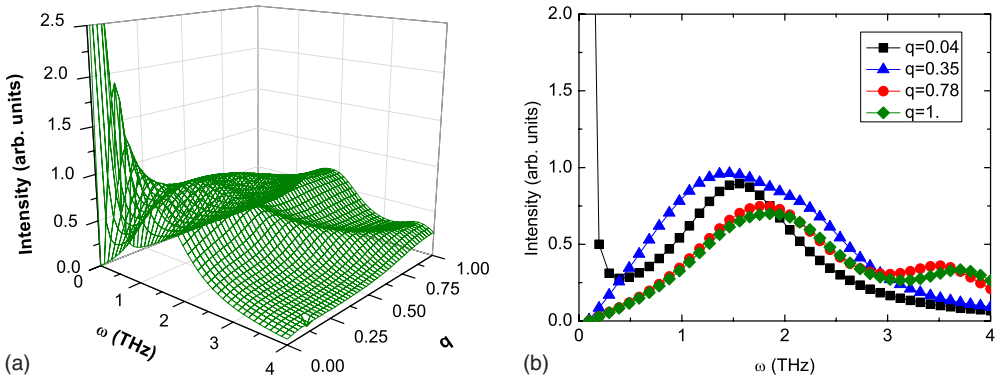

FIG. 5. (Color online) (a) Frequency and momentum dependence of the linewidth intensities of the modes shown in Fig. 2, however, well below T_B but above T_c. The ILM distribution is dense. (b) The same as in the left panel, however, showing some distinct q values as indicated in the figure.

$$\omega_1^2 = \frac{1}{m_1}\left[4f' + (2g_T + C^r\tilde{g}_4C^2)\frac{C}{A}\right], \tag{7}$$

i.e., the ILM mode becomes T dependent in an analogous way as the soft mode as long as the amplitude is small. In the vicinity of T_c substantial fluctuations in the breather mode amplitude take place caused by the nonlinear temperature dependence of C whereas for elevated temperatures an almost linear T dependence is realized. The renormalization due to this effect is shown in Fig. 3 for temperatures close to T_c where precursor type dynamical fluctuations govern the renormalized breather amplitude.

Since the acoustic zone-boundary lattice mode frequency is given by

$$\omega_{TA}^2(q = 2\pi/a) = \frac{1}{m_1}\left[4f' + \frac{2fg_T}{2f + g_T}\right] \tag{8}$$

strong acoustic-ILM mode coupling can set in with decreasing temperature and an anomalous dispersion of the elastic constants maybe a consequence.[46] For temperatures below T_c and in the dilute case, the ILM adopts a temperature dependence where—like the soft mode—hardening is expected. In the dense case, no transition will occur since—as is obvious from Eq. (4)—the attractive coupling can be fully compensated by the coupling to the ILM.

Above the Burns temperature T_B, which is defined as the temperature where the refractive index deviates from a linear in T dependence,[20] the ILM solutions remain above the frequency of acoustic phonon mode at the Brillouin-zone boundary thus giving rise to a random distribution of breathers. However, they split off from the spectrum below T_B and form in-gap coherent states which exhibit self-organized patterns. A typical shape of phonon and breather branches in the Brillouin zone is shown in Fig. 4.

It is important to emphasize that the ILM solution is realized in a spatially limited region. Obviously, optic and acoustic modes exhibit quite conventional dispersions, as observed by INS for high temperatures. There is, however, a splitting of the ILM from the optic mode close to $q=0$ (see the inset to Fig. 4) which gives rise to diffuse scattering, phonon frequency shifts, and novel features in the phonon linewidth. In order to calculate the linewidths of the above modes, the approaches of Refs. 47–49 are used where multiphonon processes are considered to become important for the phonon (j) temperature (T)-dependent linewidth. The results of these calculations are shown in Fig. 5 where the case shown in Fig. 4 is considered.

The diagram shows the intensities of the three branches of

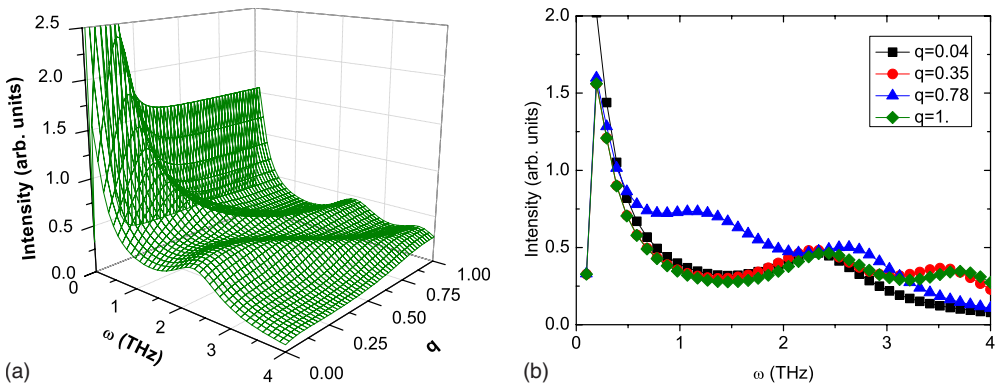

FIG. 6. (Color online) (a) Frequency and momentum dependence of the linewidth intensities of the modes shown in Fig. 4 but at a higher temperature than in Fig. 5, however still below T_B. The ILM distribution is dense. (b) The same as in the left panel, however, showing some distinct q values as indicated in the figure.

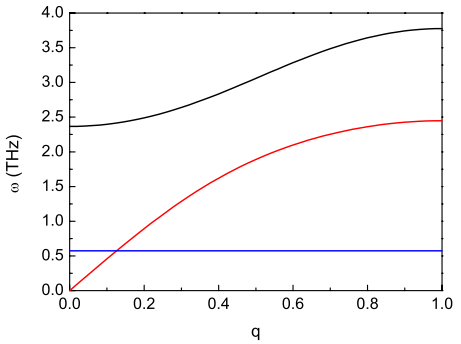

FIG. 7. (Color online) Momentum dispersion of the lowest transverse optic (black line) and acoustic mode (red line) frequencies. The blue line refers to the ILM. The ILM distribution is dilute thus leaving space for almost displacive optic mode softening.

Fig. 4 as a function of momentum q and frequency ω. These intensities are related to the dielectric loss in the $q=0$ limit. While the acoustic mode dispersion can be followed clearly in momentum space up the middle of the Brillouin zone, the optic mode is damped at small momentum and develops as a shoulder. This shoulder stems from the ILM and its interaction with the optic mode. Approaching the zone boundary, the mode damping is even more pronounced, whereas the ILM separates from the optic mode and develops an almost independent response. As can be seen, the crossing of the acoustic and the ILM modes halfway between $q=0$ and $q=2\pi/a$ leads to an additional anomaly, where both modes are no longer individually distinguishable. Note that the above case refers to a dense breather distribution at temperatures well below T_B. Upon increasing the temperature to T_B, the optic mode damping increases, its intensity decreases (Fig. 5), and the mode dispersion is followed well through the Brillouin zone. It should be underlined that such unusual increase in soft-mode damping with increased temperature was indeed observed in terahertz (THz) and IR spectra of all lead-based relaxors but only above T_B and upon approaching this temperature scale from above,[6,7,39,40] which implies that the soft-mode damping exhibits maximum at T_B.

A similar analysis has been made for the case of a dilute system (Fig. 6), where the doping and, correspondingly, the ILM amplitude are small. A typical dispersion for this case is shown in Fig. 7 where the ILM completely splits off from the optic mode and crosses the acoustic mode at small momentum. In this case the system is almost in the displacive limit and the temperature dependence of the soft mode is reminiscent of the uncoupled soft mode. This leads to a complicated frequency-dependent damping profile, where both acoustic and optic modes are overdamped with the acoustic mode showing an anomalous line-shape asymmetry (Fig. 8) caused by the coupling with the ILM.

Not only is the acoustic mode overdamped with line-shape anomalies but also the optic mode is anomalously broadened due to spectral weight transfer to the ILM. However, its dispersion can still be followed clearly through the full Brillouin zone. The dilute case, just discussed, refers to low temperatures and, as discussed above, the almost displacive limit. When increasing the temperature the ILM and the optic mode both shift to higher frequencies and the crossing between the acoustic and the ILM mode takes place at larger momentum. Since the optic mode also moves to higher frequencies, it does not show any crossing and, as already observed for the dense case, becomes well defined but strongly damped. This is shown in Fig. 9.

Experimentally it has been observed[6,7,39,40] that the soft-mode damping has a maximum at T_B and diminishes above T_B in an unexpected manner. The above results for temperatures smaller than T_B are consistent with these data. For $T>T_B$ we suggest that the incoherence of the ILM and its splitting off the phonon spectrum diminishes the damping and indeed will produce in this way the observed damping maximum at the Burns temperature. Details about the temperature evolution of the damping for $T>T_B$ will be published in another work. Also, it is worth mentioning that the dielectric relaxations below the phonon spectrum cannot be evaluated within the present approach, however, it is important to emphasize that the relaxation contribution to the permittivity is essential below T_B in relaxor ferroelectrics.

The dense and dilute cases of ILMs in a polarizable matrix have distinct effects on the temperature dependencies of all modes. With a dense distribution, the large amplitude breather stabilizes the soft-mode temperature dependence and inhibits a structural instability [Fig. 10(a)]. On the other

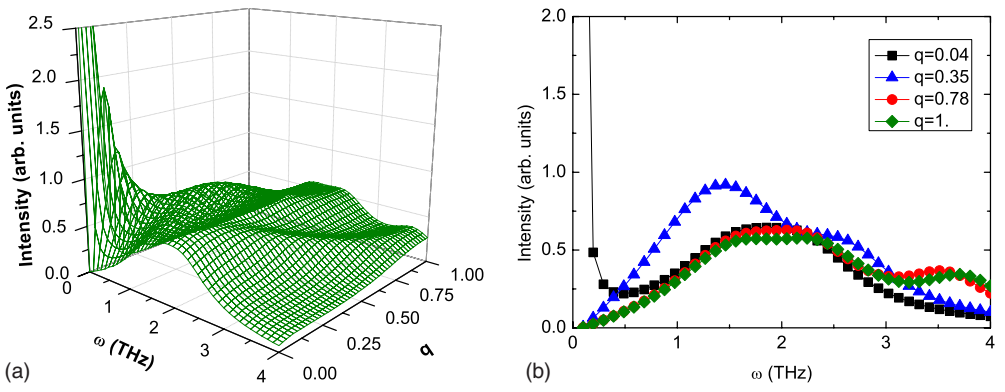

FIG. 8. (Color online) (a) Frequency and momentum dependence of the linewidth intensities of the modes shown in Fig. 7. The ILM distribution is dilute. The temperature is well below T_B but still above T_c. (b) The same as in the left panel, however, showing some distinct q values as indicated in the figure.

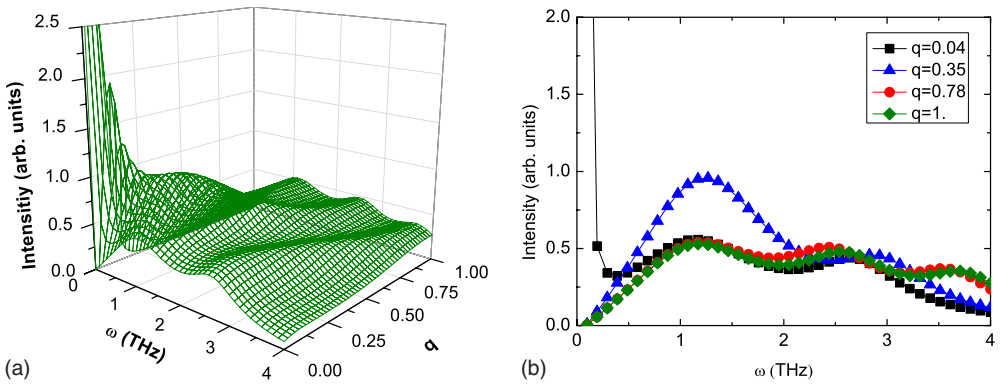

FIG. 9. (Color online) (a) Frequency and momentum dependence of the linewidth intensities of the modes shown in Fig. 7 but at a higher temperature as compared to Fig. 8, however below T_B, the ILM distribution is dilute. (b) The same as in the left panel, however, showing some distinct q values as indicated in the figure.

hand, the breather adopts a T dependence whereas the acoustic zone-boundary mode frequency which typically is also rather strongly temperature dependent, greatly decreases this T dependence and is almost pinned to a fixed value. It is, however, seen [Fig. 10(a)] that a crossing of acoustic and ILM modes takes place at intermediate temperatures, signaling the onset of increased elastic softness and the possibility for an elastic instability. In the opposite case of a dilute small amplitude ILM distribution [Fig. 10(b)], the zero-momentum optic mode shows typical softening, as observed in displacive ferroelectric systems. An instability is possible in this case which is very much reminiscent of a true ferroelectric phase transition, however with the distinction the complete mode softening is inhibited as discussed above. Also the related zone-boundary acoustic mode shows the typical displacive type temperature dependence. Near T_c, strong mode coupling of acoustic and optic modes takes place which induces an anomalous dispersion of the acoustic mode at small wave vector, which experimentally shows up as anomalies in Brillouin-zone scattering and anomalous elastic behavior.[46,50–54] The breather mode, on the other hand, is much less affected by temperature as compared to the dense case and decreases from the highest to zero temperature by only 1.22 THz (3.32 THz in the dense case).

The two limiting cases discussed above can adopt all intermediate possibilities since the ILM amplitude varies continuously with doping. This means that a smooth crossover from the purely displacive to the relaxor case is possible, as also suggested from experiments.[15,16] In the extreme dilute case, considered above, even a coexistence of relaxor and soft-mode dynamics can occur. The observation of inhomogeneous polar nanodomains, discussed here in terms of local mode formation, is not tied to T_B but is expected to be possible above T_B. At these high temperatures, coherence, which causes ILM formation, of the polar nanoregions is not yet achieved making it difficult to observe them. They should, however, be observable through local probe techniques such as NMR, PDF, or extended x-ray-absorption fine structure (EXAFS). The dynamics of the matrix are expected to be "normal." Only, when the breather frequency reaches the phonon spectrum at either the zero-momentum optic phonon or the transverse-acoustic zone-boundary mode, namely, at T_B, coherence takes place and the polar nanoregions are observable by conventional scattering techniques.

A direct probing of the continuous crossover from strong mode softening in ferroelectrics to an incomplete softening relaxor as predicted in Fig. 9 is still lacking, even though the incomplete mode softening has been observed by infrared and broadband dielectric spectroscopy in various relaxor systems.[6,7,39,40] Indeed, observing the continuous crossover would require a full set of single crystals in a solid solution [for example, the $BaTi_{1-x}Zr_xO_3$ (BTZ)] solution. Reliable IR,

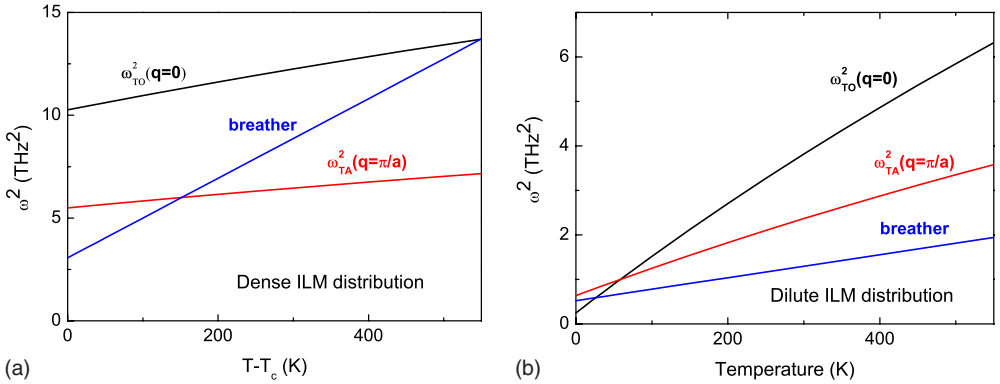

FIG. 10. (Color online) Temperature dependence of the squared optic ($q=0$; black line), acoustic ($q=\pi/a$; red line and breather ($q=0$; blue line) mode frequencies in (a) the dense ILM case and (b) the dilute ILM case.

TABLE I. Curie constants C_{CW} of several ferroelectric (F) and relaxor (R) materials in the same $BaTiO_3$ family; some other ferroelectric materials are listed for reference. T_c and T_m are the real, respectively, extrapolated transition temperatures.

Composition	T_c or T_m (K)	Curie constant C_{CW} (K)	Reference
$BaTiO_3$ (F)	400	1.5×10^5	45
$Ba(Ti_{0.85}Zr_{0.15})O_3$ (F)	340	1.5×10^5	43
$Ba(Ti_{0.80}Zr_{0.20})O_3$ (F)	314	1.6×10^5	43
$Ba(Ti_{0.63}Zr_{0.37})O_3$ (R)	194	1.06×10^5	43
$Ba(Ti_{0.60}Zr_{0.40})O_3$ (R)	188	1.03×10^5	43
$Ba_{0.88}Ca_{0.12}(Ti_{0.63}Zr_{0.37})O_3$ (R)	169	9.9×10^4	43
$Ba_{0.90}Ca_{0.10}(Ti_{0.70}Zr_{0.30})O_3$ (R)	209	8.2×10^4	43
$KNbO_3$ (F)	691	2.4×10^5	45
$PbTiO_3$ (F)	763	4.1×10^5	45
$Pb(Zn_{1/3}Nb_{2/3})O_3$ (R)	388	2.69×10^5	55, 56
$Pb(Mg_{1/3}Nb_{2/3})O_3$ (R)	265	1.25×10^5	57

Raman, and inelastic neutron scattering would then be available. Since, however, such high quality single crystals are still missing, TO phonon investigations in ceramics samples could not evidence the required slowing down.[44] An alternative way can be found in the high-temperature extrapolation of the dielectric permittivity in a set of ceramics like BTZ. Indeed, through the Lyddane-Sachs-Teller equation, the low-frequency permittivity is directly related to the TO mode softening: $\varepsilon(T)\propto[\omega_f(T)]^{-2}$ where this relation is valid for $T>T_B$ in relaxor ferroelectrics. Instead of focusing the attention to the critical temperature range where either true ferroelectric or dispersed relaxor behavior occurs, we investigated the temperature range where the Curie-Weiss law is valid in both instances,

$$\varepsilon(T)=\frac{C_{CW}}{(T-T_c)} \tag{9}$$

with C_{CW} being the Curie constant and T_c is an extrapolated temperature which loses its meaning in the case of relaxors because it is first frequency dependant and second the deviation from Eq. (9) precludes any reliable fitting of the permittivity data.

Usually, it is this deviation which is used to assign the occurrence of a relaxor state. On the basis of the breather model we will rather restrict our attention to the temperatures where Eq. (9) is valid for ferroelectrics as well as for relaxor, i.e., for the latter systems above T_B. Plotting the inverse of $\varepsilon(T)$ versus T is the correct way to evidence the Curie-Weiss law. This is done in Fig. 10 for some key compositions in the BTZ family. As the critical temperature range has been omitted in these plots, only the computed slope C_{CW} of the lines is the parameter of interest. This Curie constant is reported in Table I for several BTZ compounds together with their ferroelectric or relaxor characteristic transition temperatures.[15] In the same table typical Curie constants for $KNbO_3$ and $PbTiO_3$ ferroelectrics are also included. Obviously, the Curie constants split into two groups: the one of displacive type ferroelectrics with $C_{CW}>1.5\times10^5$ K and the one of relaxors with $C_{CW}<1.1\times10^5$ K. Even if this difference is not huge, it is systematically observed in the $BaTiO_3$ based compounds including the BaCaTiZrO ferroelectric/relaxor compositions (Table I). This is an indirect confirmation of the key model expectation of Fig. 10 calling for an incomplete softening of ω_f^2 in relaxors. The clue here is that the variation in Curie constants is quite sharp when shifting from the ferro-

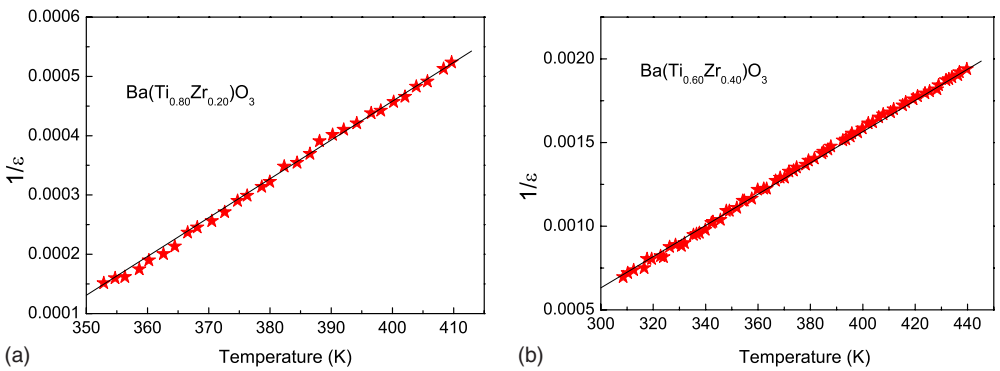

FIG. 11. (Color online) Curie-Weiss behavior of a ferroelectric $Ba(Ti_{0.80}Zr_{0.20})O_3$ and a relaxor $Ba(Ti_{0.60}Zr_{0.40})O_3$ taken from the whole family of materials reported in Table I. The lines are obtained through a fit to Eq. (9). The data have been taken at 1 THz.

electric to relaxor compositions while the critical temperatures are continuously decreasing without any sign of criticality for many lead free solid solutions.[15] This a very strong support for the breather model—whether diluted or dense—being a microscopic precursor of two different behaviors which are only macroscopically distinguishable close to the critical temperature. The agreement between these experimental findings and the model predictions becomes clear by comparing Figs. 11(a) and 11(b).

The above model for relaxor ferroelectrics and their relation to displacive ferroelectrics provides a natural explanation of many as yet unexplained phenomena. These phenomena are especially: the strong diffuse scattering, observed in all of these compounds;[10–14] the appearance of an extra mode,[6,7] in spite of missing symmetry breaking; the observation of a soft mode together with relaxor properties; the anomalous line shapes of acoustic and optic modes; and the waterfall phenomenon[9–12] and the observation of acoustic mode and elastic constant anomalies.[46,50–54]

To conclude, we have shown that relaxor and displacive dynamics are intimately related to each other and stem from the same dynamics. The strong nonlinearity, inherent to both types of ferroelectrics, gives rise to local mode formation in terms of breathers, which are intrinsically inhomogeneous and are the origin of polar nanoregions. These regions are present at all temperatures but manifest themselves only when they achieve coherence, i.e., appear in the optic-acoustic mode gap. The spatial extensions of these solutions are dependent on their amplitude related to the dopant density. In order to clearly identify them, we suggest investigating the local structure of relaxors by means of EXAFS techniques which should be able to detect the suggested patterning.

It is a pleasure to acknowledge stimulating discussions with J. Toulouse. Financial supports by the Czech Science Foundation (Project 202/09/0682) and AVOZ10100520 are gratefully acknowledged.

[1] G. Smolenski and A. Agarnovskaya, Sov. Phys. Solid State **1**, 1429 (1960).
[2] D. Viehland, S. J. Land, L. E. Cross, and M. Wuttig, J. Appl. Phys. **68**, 2916 (1990).
[3] C. Randall, Ph.D. thesis, University of Essex, 1987.
[4] L. E. Cross, Ferroelectrics **76**, 241 (1987).
[5] For a recent review see, G. A. Samara, J. Phys. Condens. Matter **15**, R367 (2003), and references therein.
[6] J. Macutkevic, S. Kamba, J. Banys, A. Brilingas, A. Pashkin, J. Petzelt, K. Bormanis, and A. Sternberg, Phys. Rev. B **74**, 104106 (2006).
[7] S. Kamba, D. Nuzhnyy, V. Bovtun, J. Petzelt, Y. L. Wang, N. Setter, J. Levoska, M. Tyunina, J. Macutkevic, and J. Banys, J. Appl. Phys. **102**, 074106 (2007).
[8] S. Tsukada and S. Kojima, Phys. Rev. B **78**, 144106 (2008).
[9] P. M. Gehring, S. Wakimoto, Z.-G. Ye, and G. Shirane, Phys. Rev. Lett. **87**, 277601 (2001).
[10] P. M. Gehring, S.-E. Park, and G. Shirane, Phys. Rev. B **63**, 224109 (2001).
[11] P. M. Gehring, S.-E. Park, and G. Shirane, Phys. Rev. Lett. **84**, 5216 (2000).
[12] P. M. Gehring, H. Hiraka, C. Stock, S.-H. Lee, W. Chen, Z.-G. Ye, S. B. Vakhrushev, and Z. Chowdhuri, Phys. Rev. B **79**, 224109 (2009).
[13] J. Hlinka, S. Kamba, J. Petzelt, J. Kulda, C. A. Randall, and S. J. Zhang, Phys. Rev. Lett. **91**, 107602 (2003).
[14] W. Dmowski, S. B. Vakhrushev, I.-K. Jeong, M. P. Hehlen, F. Trouw, and T. Egami, Phys. Rev. Lett. **100**, 137602 (2008).
[15] A. Simon, J. Ravez, and M. Maglione, J. Phys. Condens. Matter **16**, 963 (2004).
[16] M. Tyunina and J. Levoska, Phys. Rev. B **70**, 132105 (2004).
[17] J. Toulouse, P. DiAntonio, B. E. Vugmeister, X. M. Wang, and L. A. Knauss, Phys. Rev. Lett. **68**, 232 (1992).
[18] J. Toulouse and B. Hennion, Phys. Rev. B **49**, 1503 (1994).
[19] B. Burton, Phase Transitions **79**, 91 (2006).
[20] G. Burns and F. H. Dacol, Solid State Commun. **48**, 853 (1983).
[21] V. Westphal, W. Kleemann, and M. D. Glinchuk, Phys. Rev. Lett. **68**, 847 (1992).
[22] R. Blinc, J. Dolinsek, A. Gregorovic, B. Zalar, C. Filipic, Z. Kutnjak, A. Levstik, and R. Pirc, Phys. Rev. Lett. **83**, 424 (1999).
[23] R. Blinc, V. Laguta, and B. Zalar, Phys. Rev. Lett. **91**, 247601 (2003).
[24] B. E. Vugmeister and P. Adhikari, Ferroelectrics **157**, 341 (1994).
[25] B. E. Vugmeister and M. D. Glinchuk, Rev. Mod. Phys. **62**, 993 (1990).
[26] J. Toulouse, B. E. Vugmeister, and R. Pattnaik, Phys. Rev. Lett. **73**, 3467 (1994).
[27] A. Bussmann-Holder and A. R. Bishop, Phys. Rev. B **70**, 184303 (2004).
[28] A. Bussmann-Holder, A. R. Bishop, and T. Egami, Europhys. Lett. **71**, 249 (2005).
[29] A. Bussmann-Holder and A. R. Bishop, J. Phys. Condens. Matter **16**, L313 (2004).
[30] R. Migoni, H. Bilz, and D. Bäuerle, Phys. Rev. Lett. **37**, 1155 (1976).
[31] H. Bilz, G. Benedek, and A. Bussmann-Holder, Phys. Rev. B **35**, 4840 (1987).
[32] M. Stachiotti and R. Migoni, J. Phys. Condens. Matter **2**, 4341 (1990).
[33] M. Stachiotti, R. Migoni, and U. Höchli, J. Phys. Condens. Matter **3**, 3689 (1991).
[34] A. Bussmann-Holder, H. Bilz, and G. Benedek, Phys. Rev. B **39**, 9214 (1989).
[35] G. Benedek, A. Bussmann-Holder, and H. Bilz, Phys. Rev. B **36**, 630 (1987).
[36] A. Bussmann-Holder, A. R. Bishop, and G. Benedek, Phys. Rev. B **53**, 11521 (1996).
[37] A. Bussmann-Holder and A. R. Bishop, Phys. Rev. B **56**, 5297 (1997).
[38] I.-K. Jeong, Phys. Rev. B **79**, 052101 (2009).

[39] S. Kamba, M. Kempa, V. Bovtun, J. Petzelt, K. Brinkman, and N. Setter, J. Phys. Condens. Matter **17**, 3965 (2005).
[40] J. Hlinka, J. Petzelt, S. Kamba, D. Noujni, and T. Ostapchuk, Phase Transitions **79**, 41 (2006).
[41] J. Toulouse, F. Jiang, O. Svitelskiy, W. Chen, and Z.-G. Ye, Phys. Rev. B **72**, 184106 (2005).
[42] R. Farhi, M. El Marssi, A. Simon, and J. Ravez, Eur. Phys. J. B **9**, 599 (1999).
[43] J. Ravez, C. Broustera, and A. Simon, J. Mater. Chem. **9**, 1609 (1999).
[44] A. Simon (private communication).
[45] T. Mitsui and S. Nomura, *Ferroelectrics and related substances*, Landolt Börnstein (Springer-Verlag, Berlin, New York, 1981).
[46] S. G. Lushnikov, A. I. Fedoseev, S. N. Gvasaliya, and S. Kojima, Phys. Rev. B **77**, 104122 (2008).
[47] A. A. Maradudin and A. E. Fein, Phys. Rev. **128**, 2589 (1962).
[48] P. G. Klemens, Phys. Rev. **148**, 845 (1966).
[49] M. Balkanski, R. F. Wallis, and E. Haro, Phys. Rev. B **28**, 1928 (1983).
[50] R. Laiho, S. G. Lushnikov, S. D. Prokhorova, and I. G. Siny, Sov. Phys. Solid State **32**, 2024 (1990).
[51] I. G. Siny, S. G. Lushnikov, C.-S. Tu, and V. H. Schmidt, Ferroelectrics **170**, 197 (1995).
[52] S. G. Lushnikov, J.-H. Ko, and S. Kojima, Appl. Phys. Lett. **84**, 4798 (2004).
[53] M. Ahart, A. Asthagiri, Z.-G. Ye, P. Dera, H.-K. Mao, R. E. Cohen, and R. J. Hemley, Phys. Rev. B **75**, 144410 (2007).
[54] G. A. Smolenski, N. K. Yushin, and S. I. Smirnov, Sov. Phys. Solid State **27**, 801 (1985).
[55] G. Burns and F. H. Dacol, Phys. Rev. B **28**, 2527 (1983).
[56] A. E. Glazounov and A. K. Tagantsev, Appl. Phys. Lett. **73**, 856 (1998).
[57] D. Viehland, S. J. Jang, L. E. Cross, and M. Wuttig, Phys. Rev. B **46**, 8003 (1992).